Article:
Li, G-J., Zhu, Z-Q. and Jewell, G. (2015) Performance investigation of hybrid excited switched flux permanent magnet machines using frozen permeability method. IET Electric Power Applications, 9 (9). pp. 586-594. ISSN 1751-8660

https://doi.org/10.1049/iet-epa.2015.0129

Performance Investigation of Hybrid Excited Switched Flux PM Machines using Frozen Permeability Method

Guang-Jin Li*, Zi-Qiang Zhu, Fellow, IET, and Geraint Jewell

Department of Electronic and Electrical Engineering, University of Sheffield, Sheffield, UK

g.li@sheffield.ac.uk

Abstract — This paper investigates the electromagnetic performance of a hybrid excited switched flux permanent magnet (SFPM) machine using the frozen permeability (FP) method. The flux components due to PMs, field excitation windings and armature windings have been separated using the FP method. It has been used to separate the torque components due to the PMs and excitations, providing a powerful insight into the torque generation mechanism of hybrid excited SFPM machines. It also allows the accurate calculation of d- and q-axis inductances, which will then be used to calculate the torque, power and power factor against rotor speed to compare the relative merits of hybrid excited SFPM machines with different types of PMs (i.e. NdFeB, SmCo and Ferrite). This offers the possibility of choosing appropriate PMs for different applications (maximum torque or maximum speed). Although only one type of hybrid excited PM machine has been employed to carry out the investigations, the method used in this paper can also be extended to other hybrid excited PM machines. The predicted results have been validated by tests.

1. INTRODUCTION

SWITCHED flux permanent magnet (SFPM) machines are increasingly being investigated both in academia and in industry. This is mainly due to their inherent advantages such as simple and robust rotor structure, similar to that of switched reluctance machine, and hence very suitable for safety-critical applications [1]-[3]; all active parts (armature windings and magnets) are located on the stator, making their cooling much easier than the rotor mounted PM machines [4]-[5]; the PMs are sandwiched by two U-shaped stator iron cores, leading to bipolar flux linkage and hence higher torque density than other stator mounted PM machines such as that with PMs in stator yoke [6]; V-shaped PMs, similar to that of V-shaped interior PM machines, leading to flux focusing effect, and hence low cost PMs can be used to produce the desired torque density. To extend the range of application for SFPM machines, considerable amount of effort has been made to develop new topologies in recent years, and new E-core and C-core SFPM machines have been proposed and are still being intensively investigated [7]-[8].

However, due to the shortage and the high price of rare earth materials, looking for alternatives of PMs becomes more and more urgent. To cope with this challenge, wound field (magnets free) switched flux machines have been proposed, which also provide another outstanding characteristic, i.e. flux weakening capability [9]-[11]. Compared to SFPM machines, in which the open-circuit

flux due to PMs is difficult to be reduced using the demagnetizing d-axis current, the open-circuit flux linkage of wound field switched flux machines can be weakened simply by reducing the dc current, and hence have theoretically infinite flux weakening capability. Nevertheless, the maximum torque capability of wound field switched flux machines is often compromised due to thermal limitations because both armature and field windings contribute to relatively high copper loss.

In order to balance the flux weakening and the maximum torque capacities [12], hybrid excited structures developed from single excited (PMs only) SFPM machine have been proposed in recent years [13]-[15], as shown in Fig. 1, in which the excitation windings are located on top of the PMs. Other similar hybrid excited SFPM machines, in which the field windings are wound below the PMs [16] or around the PMs [17], have been proposed for HEV/EV applications. In order to minimize the influence of field winding on PMs, in particular, the field winding overheating, [18] has moved the field windings to the unwound teeth of an E-core SFPM machine or put into the armature winding slots [19]-[20], giving another alternative to hybrid excited SFPM machines. Although previous works have successfully predicted the flux weakening and flux enhancing effects due to the additional field windings, the investigation such as to which extent the field windings contribute to flux weakening or flux enhancing has rarely been carried out. To fill this gap, this paper will employ a well-established method, that is frozen permeability (FP) method, to separate the field due to PMs, field excitation windings and armature windings for both open-circuit and on-load conditions. The FP method is widely used in permanent magnet machines to separate torque components produced by permanent magnets and armature currents, because it allows taking into account of the magnetic saturation and cross-coupling [21]-[24]. As will be detailed in this paper, the FP method can also precisely predict the percentage of flux produced by field windings and PMs, giving an insight into the real nature of flux weakening or enhancing due to hybrid excitation. Since the flux due to armature and field windings as well as PMs can be separated using FP, the d- and q-axis inductances can be calculated accurately, so do the torque, power and power factor against speed characteristics.

Therefore, this paper is organized as follows: the features of a typical hybrid excited SFPM machine are summarized in section 2. Torque separation using FP method is carried out for different current angles and phase root-mean-square (RMS) currents, and a comparison in terms of average torque against excitation current has been carried out for different magnet materials in section 3. The torque, power and power factor against speed characteristics have been investigated and compared for different magnets in section 4. Tests have been carried out in section 5.A general conclusion is given in section 6.

2. Features of Hybrid Excitation SFPM Machines

A. Topologies

The typical structure of the hybrid excited SFPM machine that will be used to carry out the investigations is shown in Fig. 1 (a) [13]. This machine has 12 stator slots and 10 rotor poles. Its 12 field coils connected in series, will be employed to provide magnetic field for both flux weakening and enhancing operations. However, there are 12 armature coils, 4 coils amongst which are connected in series to form 1 armature phase winding for a 3-phase system. The coil connections for maximum phase electromotive force (EMF) for different slot/pole number combinations can refer to the theory developed in [25]. The main parameters of the investigated machine are given in TABLE I while key characteristics of the permanent magnet materials used to the comparison purpose are given in TABLE II. If it has not been specifically pointed out, then throughout this paper, the PMs used are NdFeB. Meanwhile, to avoid confusion, the "open-circuit" means the armature windings are open-circuited.

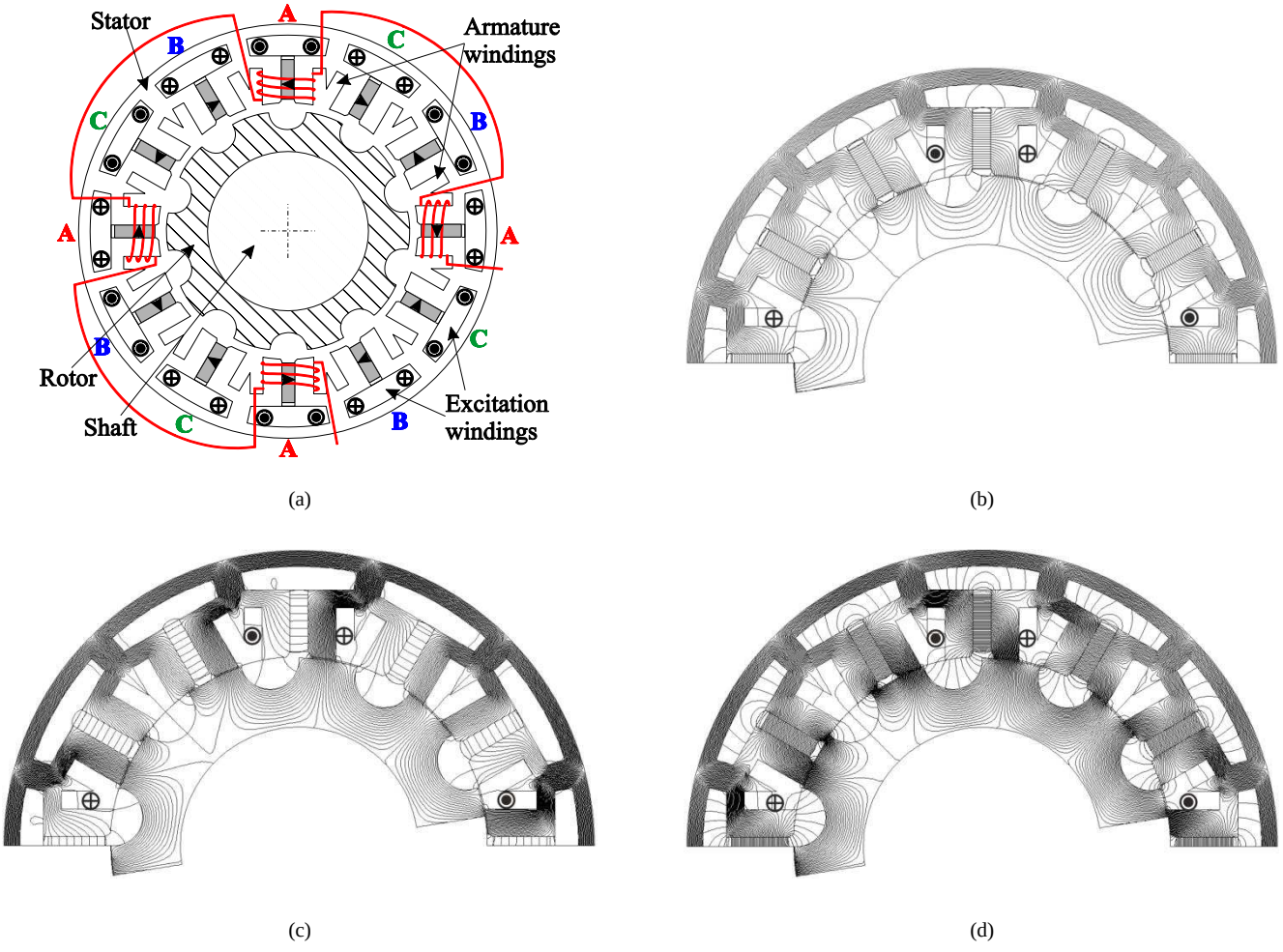

Fig. 1 Cross-section of 12-slot/10-pole hybrid excited SFPM machine, and d-axis flux line distributions with armature windings open-circuited. Magnets used are NdFeB and I_{ex} = -8A. (a) cross section, (b) flux due to I_{ex} + PMs (without FP), (c) flux due to I_{ex} only (with FP), (d) flux due to PMs only (with FP). Cross means GO conductor while dot means RETURN conductor in the figure.

TABLE I Parameters of investigated hybrid excited SFPM machine

Stator slot number	12	Number of turns of excitation	480
Rotor pole number	10	Armature phase resistance	0.52 Ω
Stator outer radius	65 mm	Excitation phase resistance	0.81 Ω
Rotor outer radius	40 mm	RMS rated armature current	7 A
Stack length	30 mm	Rated excitation current	8 A
Air-gap length	0.3 mm	DC link voltage	72 V
Number of turns per phase	148		

TABLE II Key parameters of magnet materials

	Remanence B_r (T)	Coercivity H_c (kA/m)
NdFeB	1.2	-909
SmCo	0.8	-640
Ferrite	0.4	-284

B. Flux plots and flux linkages

The FP method are often used in PM machines to separate the flux produced by armature windings and PMs, allowing for calculating the on-load electromotive force (EMF) and on-load cogging torque [23]-[24], [26]-[27]. The principle of FP method has been summarized as shown in Fig. 2 (a) and can be simply described as follows [27]:

(1) Non-linear calculation using static finite element (FE) method is carried out for a given load conditions and for different rotor positions;

(2) The relative permeability in all mesh elements of the FE model for the load conditions in (1) are then saved and frozen. This can make sure the magnetic saturation level and the working point of magnets are unchanged when load condition changes;

(3) Using the same machine geometry (FE model) but with previously saved and frozen permeability, the flux (or on-load EMF due to PMs can be calculated by resetting the armature current and excitation current to zero, or flux due to excitation current can be calculated by resetting the magnet remenance B_r and armature current to zero.

The similar FP method has been implemented to a FE model based on a commercial software (Opera 2D), and the open-circuit flux linkages due to PMs and field windings of the hybrid excited SFPM machine have been separated and compared in Fig. 1 and Fig. 2, in which the rotor position is for the phase A (cross and dot conductors) having its maximum flux linkage. It is found that when the excitation current I_{ex} = -8A, both the PMs and wound field contribute to open-circuit flux linkage. Moreover, due to a negative (demagnetizing) excitation current, the resultant flux linkage has been reduced. When I_{ex} = 8A, solely field winding

contributes to phase flux because PMs are short-circuited by stator yoke, indicating that the only effect of PMs is to saturate the stator yoke. However, without PMs, most flux produced by the field winding will be short-circuited by stator yoke and will not cross the air-gap, leading to much lower phase flux linkage as proven by [28]-[29].

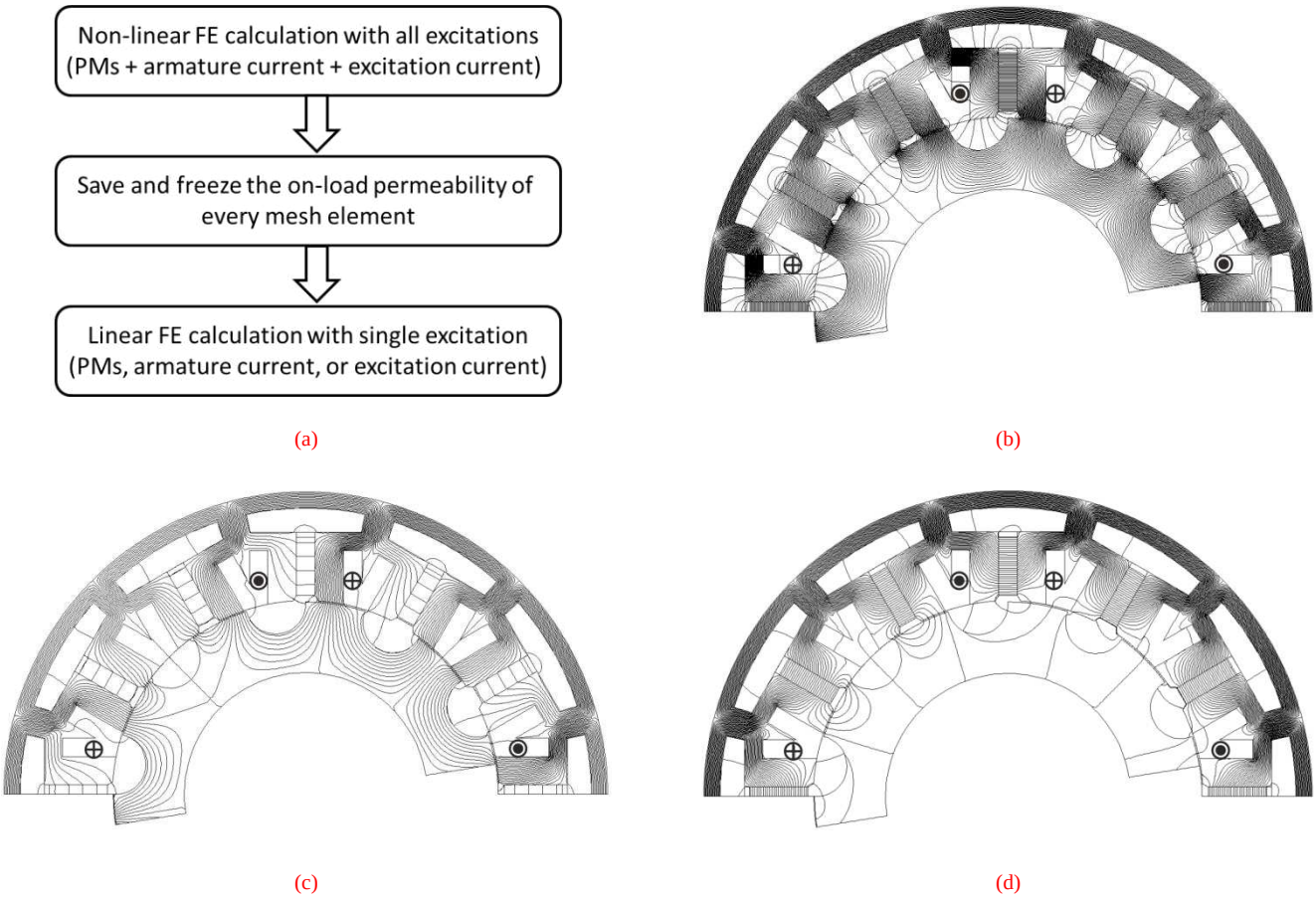

Fig. 2 d-axis flux line distributions with armature windings open-circuited. Magnets used are NdFeB and I_{ex} = 8A. (a) Implementation procedure of the conventional frozen permeability method for each rotor position [27], (b) I_{ex} + PMs (without FP), (c) I_{ex} only (with FP), (d) PMs only (with FP).

The different open-circuit flux linkage components [wound field only (I_{ex} only), magnets only (PM only), magnets + wound field (PM + I_{ex})] have been calculated using the FP method for a range of excitation current from -8A to 8A, as shown in Fig. 3. Moreover, the accuracy of the FP method has been verified by comparing the resultant flux linkage obtained with or without FP method (no FP means the flux linkage is calculated directly using FE method while with FP, the resultant flux linkage is the sum of flux linkages due to PMs and wound field). It is found that the open-circuit flux linkage due to PMs is reducing with the increase in excitation current, and can eventually become negative if the excitation current is around 8A. As a result, the flux linkage due to excitation current can be even higher than the resultant flux linkage.

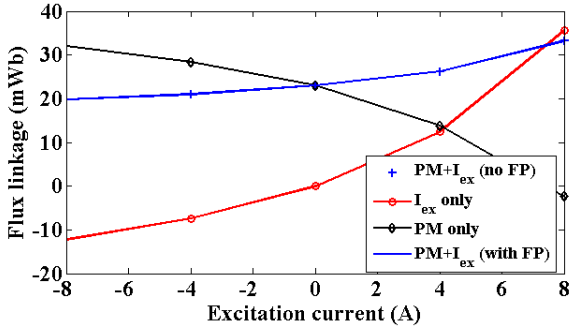

Fig. 3 Open-circuit armature winding flux linkage components separated using FP method for different excitation currents.

C. d- and q-axis inductances

The FP method can also be used to calculate the d- and q-axis inductances, which allows to accounting for the influence of d- and q-axis currents on flux linkage due to PMs + field windings, leading to more accurate estimation of d- and q-axis inductances [30]. The d- and q-axis fluxes for different phase RMS currents and excitation currents have been calculated, and using the equations (1) and (2), the d- and q-axis inductances can be calculated, as shown in Fig. 4. It is found that at low current level, the d-axis inductance is increasing with the increase in phase RMS current (relevant d-axis current) and excitation current. However, it will eventually reduce at high phase RMS current and excitation current. This is mainly due to the heavy magnetic saturation in d-axis caused by both currents. The q-axis inductance remains largely constant when phase RMS current (relevant q-axis current) increases while increases with the increase in excitation current. These variations in d- and q-axis inductances will have a significant impact on the machine performance, in particular the flux weakening capability, as will be detailed in section 4.

$$\begin{cases} \Phi_d = \left(\Phi_{d\_pm} + \Phi_{d\_ext}\right)_{FP} + L_d I_d \\ \Phi_q = \left(\Phi_{q\_pm} + \Phi_{q\_ext}\right)_{FP} + L_q I_q \end{cases} \tag{1}$$

Therefore, the d- and q-axis inductances can be calculated by

$$\begin{cases} L_d = \dfrac{\Phi_d - \left(\Phi_{d_{pm}} + \Phi_{d_{ext}}\right)_{FP}}{I_d} \\ L_q = \dfrac{\Phi_q - \left(\Phi_{q_{pm}} + \Phi_{q_{ext}}\right)_{FP}}{I_q} \end{cases} \tag{2}$$

where $\left(\Phi_{(d\ or\ q)\_pm}\right)_{FP}$ and $\left(\Phi_{(d\ or\ q)\_ext}\right)_{FP}$ are the on-load d- or q-axis flux linkages due to PMs and field windings, respectively, which are obtained by using FP method when d- and q-axis currents are supplied. I_d and I_q, L_d and L_q are the d- and q-axis currents, and inductances, respectively.

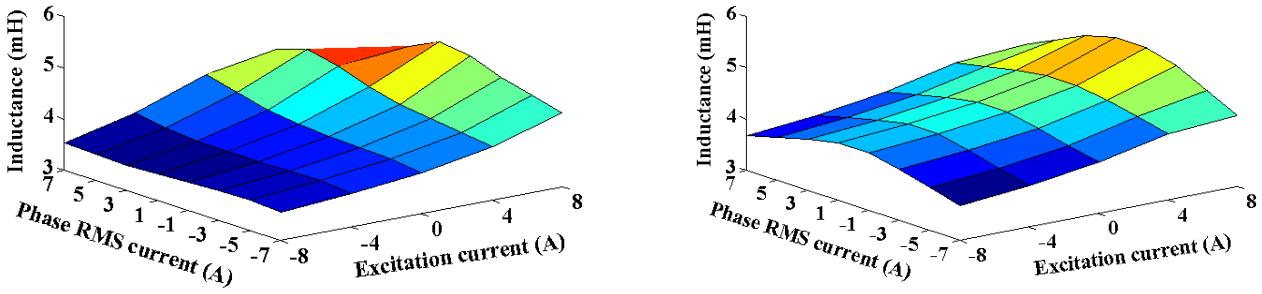

(a) (b)

Fig. 4 d- and q-axis inductances vs phase RMS currents and excitation currents. (a) L_d (current phase advanced angle = 0 Elec. Deg), (b) L_q (current phase advanced angle = 90 Elec. Deg).

3. TORQUE SEPARATION USING FP METHOD

The field winding of hybrid excited SFPM machines, due to its capability of flux enhancing and flux weakening, will have a profound impact on machines' torque capability, as will be detailed in this section.

A. On-Load Torques

Without accounting for cogging torque, the general torque equation of the hybrid excited SFPM machines can be described by

$$T = \frac{3}{2} p \left[\left(\Phi_{d\_pm} + \Phi_{d\_ext} \right)_{FP} I_q + \left(L_d - L_q \right) I_d I_q \right] \tag{3}$$

where $\frac{3}{2} p \left[\left(\Phi_{d\_pm} + \Phi_{d\_ext} \right)_{FP} I_q \right]$ is excitation torque due to PMs and field windings while $\frac{3}{2} p \left(L_d - L_q \right) I_d I_q$ is the reluctance torque. Therefore, the field winding will mainly influence the excitation field and hence the excitation torque. However, its influence on reluctance torque is mainly due to saturation effect.

Using FP method, the torque components such as torque due to wound field (T_{Iex}), torque due to PMs (T_{PM}), reluctance torque (T_{rel}) and the resultant torque [T_{vir}(with FP), equals to $T_{Iex} + T_{PM} + T_{rel}$] have been calculated for different phase advanced angles, as shown in Fig. 5. It is worth noting that when the FP method is used to separate torque components, the Virtual Work method should be used to calculate torque because the classic method such as Maxwell Stress Tensor is not accurate anymore, as proven in [24]. However, without employing the FP method, the Maxwell Stress Tensor can be used to directly calculate the resultant torque [T_{mw}(no FP)]. This allows to verifying the accuracy of torque separation method using FP as T_{mw}(no FP) matches perfectly with T_{vir}(with FP) for different phase advanced angle and excitation currents.

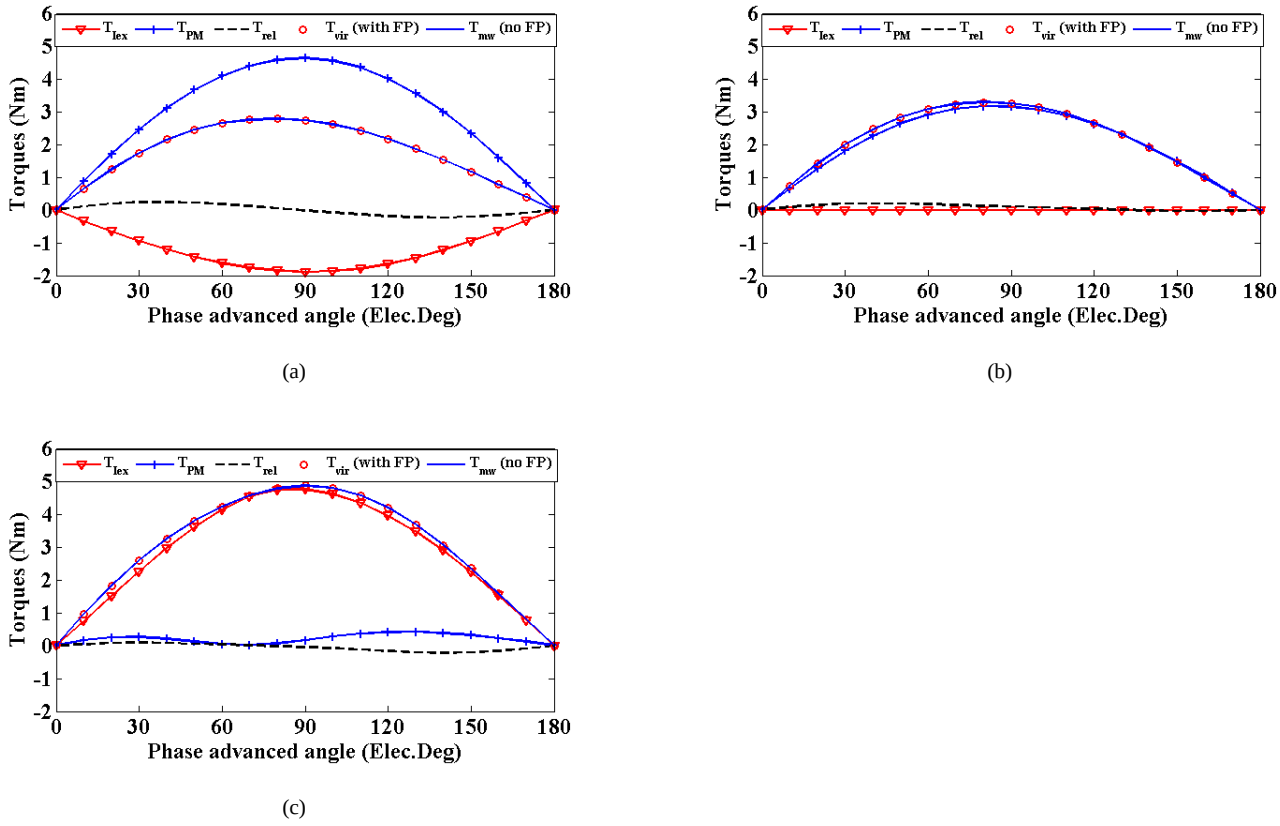

Fig. 5 On-load torque components vs armature current phase advanced angle obtained by using FP method. The armature RMS current is 7 A. (a) I_{ex} = -8A, (b) I_{ex} = 0A, (c) I_{ex} = 8A. 0 Elec. Deg is where phase A has maximum flux linkage (d-axis).

It is also found that, for the full range of phase advanced angle and excitation current, the reluctance torques, as in the case of single excited SFPM machines, are considerably low and negligible. However,

- For I_{ex} = -8A, T_{Iex} is negative, leading to a reduction in T_{vir}(with FP).
- For I_{ex} = 0A, T_{Iex} is null and T_{PM} is the predominant torque component.
- For I_{ex} = 8A, T_{PM} as T_{rel}, is negligible, this is mainly due to the fact that the fluxes due to PMs do not cross the air-gap as shown in Fig. 2 (c) and will not contribute to torque production. Therefore, T_{Iex} is the predominant torque component.

As shown in Fig. 5, the maximum resultant torques for different excitation currents can be obtained when the phase advanced angle is around 90 elec. deg. Therefore, this angle is chosen to calculate the average torques against phase RMS current, as shown in Fig. 6. Again, the resultant torque has been calculated by both the virtual work method and the Maxwell stress tensor method to verify the accuracy of the torque separation method using FP. It has been found that for a negative excitation current I_{ex} = -8A, the torque due to excitation only is always negative, leading to a reduction in resultant torque. When I_{ex} = 0A, the resultant torque is only produced by the PMs since the reluctance torque is neglected. When I_{ex} = 8A, as shown in Fig. 5 (c), the torque due to PMs is

largely negligible for the full range of phase RMS current, leading to a resultant torque mainly determined by the torque component due to excitation.

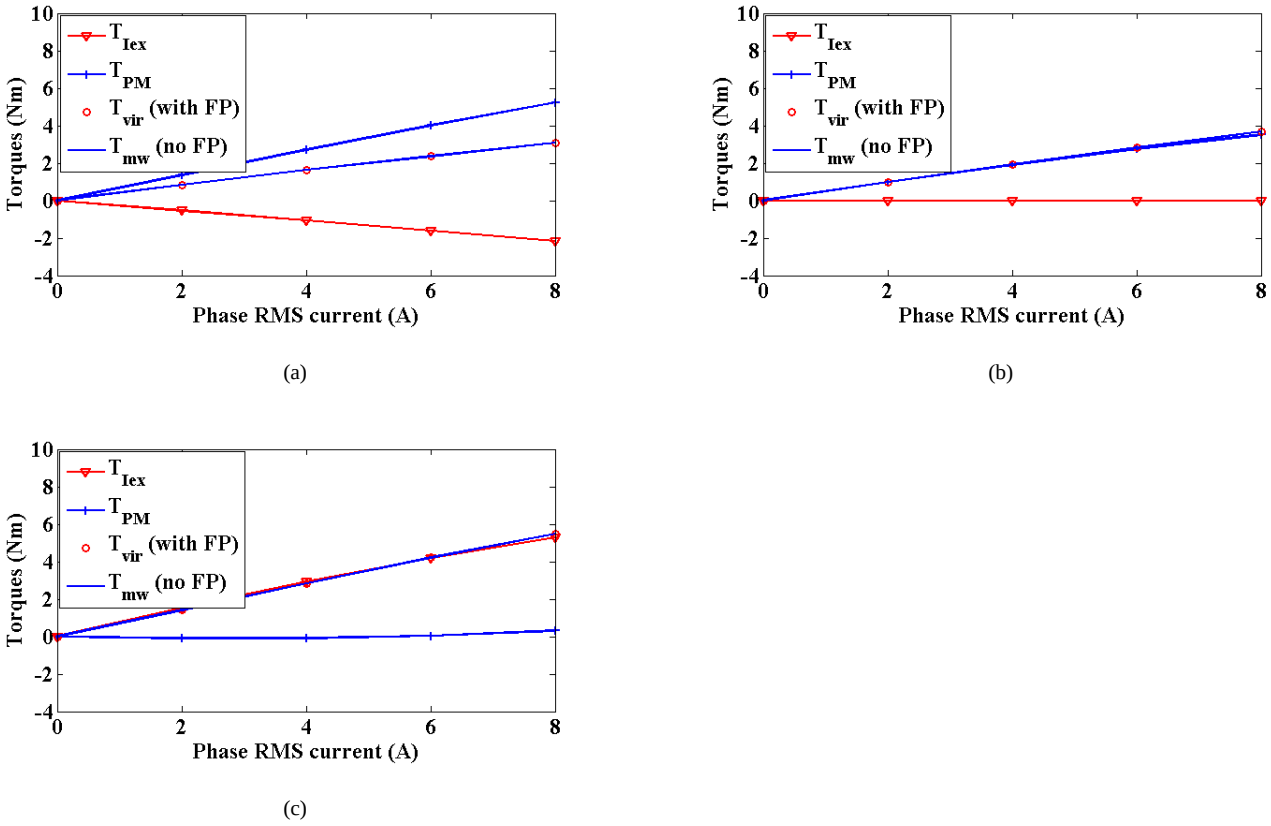

(a) (b)

(c)

Fig. 6 On-load torque components vs armature phase RMS current obtained by using FP method. The armature current phase advanced angle is 90 Elec. Deg. (a) I_{ex} = -8A, (b) I_{ex} = 0A, (c) I_{ex} = 8A.

B. Torque Comparison for Different PMs

Still fixing the current phase advanced angle to 90 elec. deg. the torques against excitation current for hybrid excited SFPM machines with different magnets have been calculated using FP method and compared in Fig. 7. It is found that the machine using Ferrite produces the lowest resultant torque for the full range of excitation current with the SmCo being the second lowest. However, when the excitation current is around 8A, the machines with SmCo and NdFeB produce similar resultant torque but the SmCo has much lower remanence as shown in TABLE II. It is also important to find out that the torque due to excitation only is nearly independent of PM types. However, when it comes to the torque component due to PMs only, which reduces for all PMs with the increase in excitation current. Nevertheless, the reduction in PM torque for the hybrid excited SFPM machine is the most significant, leading to a similar PM torque at high excitation current (around 8A). This means that at high excitation current, the Ferrite can be used to achieve comparable level of PM and resultant torques while maintaining much lower price level than SmCo and NdFeB.

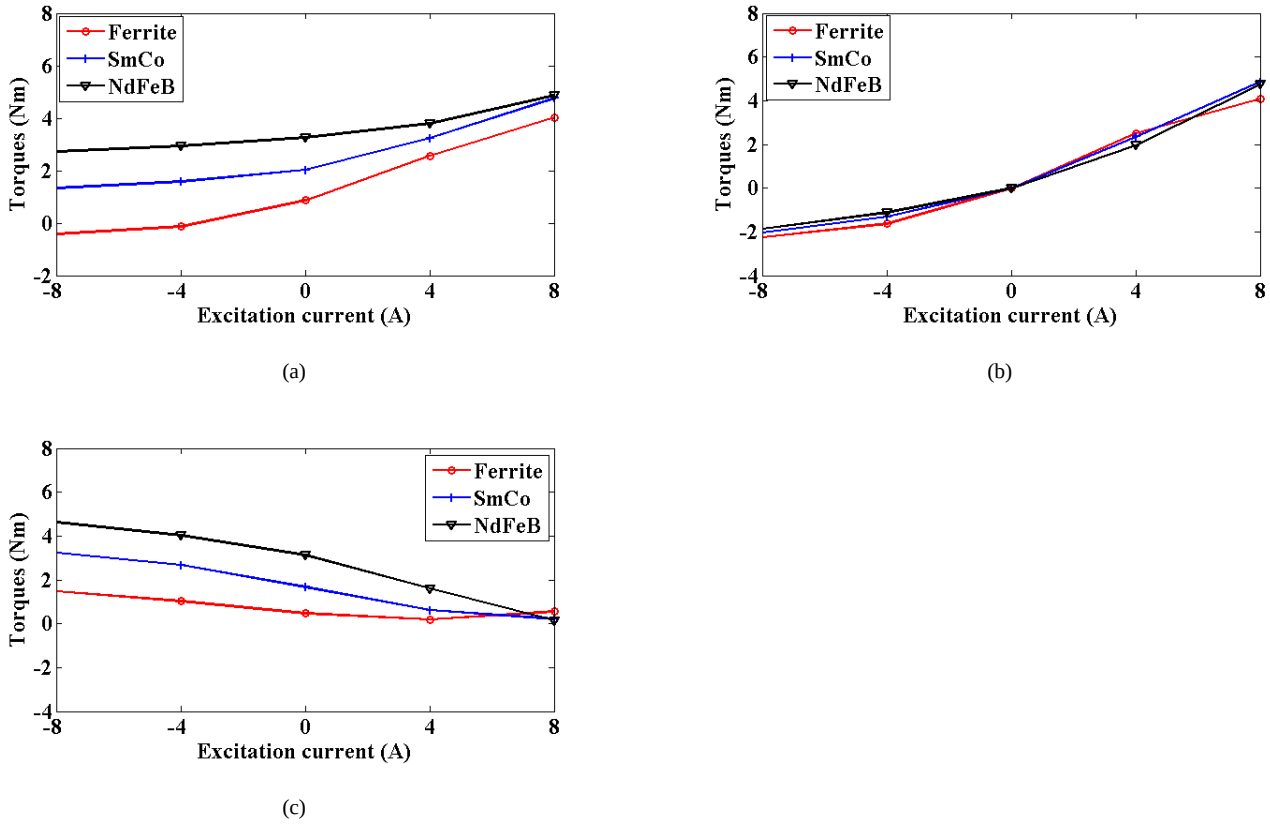

Fig. 7 Torque components vs excitation current for hybrid excited SFPM machines using different PMs. Armature current phase advanced angle is 90 Elec. Deg. and the RMS current is 7 A. (a) Resultant torque, (b) Excitation torque only, (c) PM torque only.

4. TORQUE, POWER AND POWER FACTOR AGAINST SPEED CHARACTERISTICS

The major advantage of hybrid excited PM machines over their solely PM excited counterparts is the flux weakening capability, which is one of the key requirements for EV/HEV applications. This is mainly due to the fact that the extra field winding adds another degree of freedom under flux weakening operation. As a result, not only the demagnetizing d-axis current but also a negative excitation current can be employed to reduce the armature phase flux linkage. This allows for extending the constant power range as well as reaching the maximum speed without violating the maximum current and voltage constraints of power electronic devices. Therefore, under flux weakening operation, the maximum output torque is determined by the phase voltage (U_{max}) and current (I_{max}) limits such as

$$U = \sqrt{U_d^2 + U_q^2} \le U_{max} \tag{4}$$

$$I = \sqrt{I_d^2 + I_q^2} \le I_{max} \tag{5}$$

With

$$U_d = -\omega L_q I_q + R I_d \tag{6}$$

$$U_q = \omega \left[\left(\Phi_{d\_pm} + \Phi_{d\_ext} \right)_{FP} + L_d I_d \right] + R I_q \tag{7}$$

where U_d, U_q, R and ω are d- and q-axis voltages, phase resistance and rotor electrical speed, respectively. Other parameters such as L_d, L_q and $\left(\Phi_{d\_pm} + \Phi_{d\_ext} \right)_{FP}$ can be calculated using the previously introduced FP method.

The phase current limit is determined by the maximum phase current, e.g. rated armature current is used in this paper. However, the voltage limit depends on the DC link voltage (U_{DC}) and the employed control method. When a hysteresis pulse-width modulated controller is employed [31]-[32]

$$U_{max} = \frac{2}{\pi} U_{DC} \tag{8}$$

Using the equations from (3) to (8), the flux weakening characteristics of hybrid excited SFPM machines can be analysed, as will be detailed in the following sections.

A. NdFeB PMs

By way of example, the torque, power and power factor against speed have been calculated for different excitation currents, as shown in Fig. 8. The magnets used for these calculations are NdFeB. It can be found that there is a significant extension of base speed when the excitation current changes from 8A to 0A, whilst the base speed increases slightly when the excitation current keeps reducing to -8A. This means that the excitation current has more important influence on flux enhancing than on flux weakening [29], as shown in Fig. 3. This also explains why the constant torque drops more significantly from I_{ex} = 8A to I_{ex} = 0A than from I_{ex} = 0A to I_{ex} = -8A. At high speed, the torques for different excitation currents become closer and closer, meaning that the negative excitation current can extend the maximum speed range, as expected.

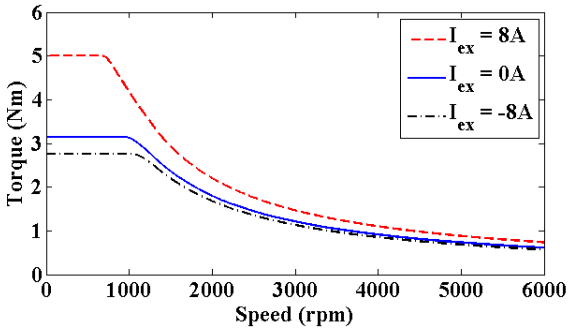

(a)

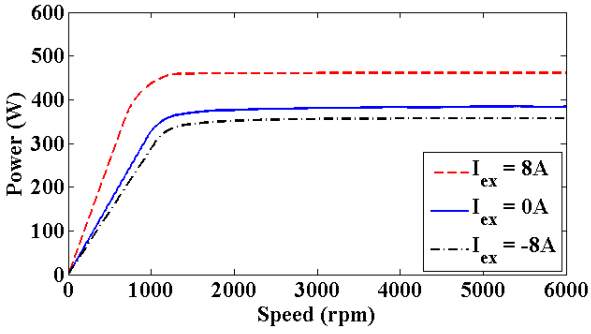

(b)

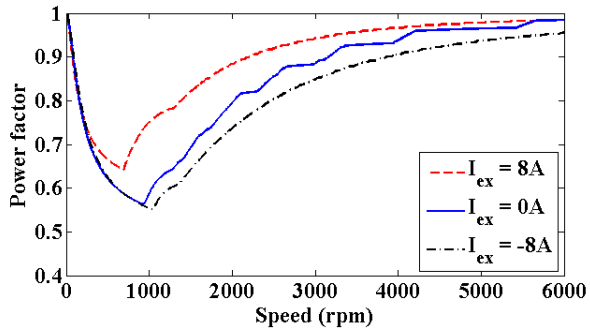

(c)

Fig. 8 Torque, power and power factor against speed characteristics for different excitation currents. The magnet is NdFeB. (a) torque, (b) power, (c) power factor. The peak armature RMS current is 7A.

The maximum power reduces with the reduction in excitation current. Again, from I_{ex} = 8A to I_{ex} = 0A, the reduction in power is more significant than from I_{ex} = 0A to I_{ex} = -8A. This is similar to the power factor at low rotor speed around 1000 rpm. However, the power factors are similar for different excitation currents at high speed $\geq$ 6000 rpm. This means that with a proper excitation current, the flux weakening can be easily achieved using hybrid excitation while the power quality can still be maintained.

B. Different PMs

Similar studies have been carried out for hybrid excited SFPM machines using different magnets (Ferrite, SmCo and NdFeB, the key characteristics of which are described in TABLE II). By way of example, the results for a fixed excitation current of 8A and a maximum phase RMS current of 7A are compared in Fig. 9. It can be found that although the NdFeB has the highest remanence, the SmCo can still produce the highest maximum torque due to a non-negligible reluctance torque (SmCo and NdFeB have similar PM + Excitation torque as shown in Fig. 7). The Ferrite has the lowest maximum torque but highest base speed due to lower PM + Excitation flux linkage. However, the torques for different PMs at high speed around 6000 rpm become similar. The NdFeB has the highest maximum power while the power factors are similar for all three PMs and for the full range of speed. This means that the Ferrite could be used as an alternative because it can produce comparable torque, power and power factor while has much lower price than NdFeB and SmCo.

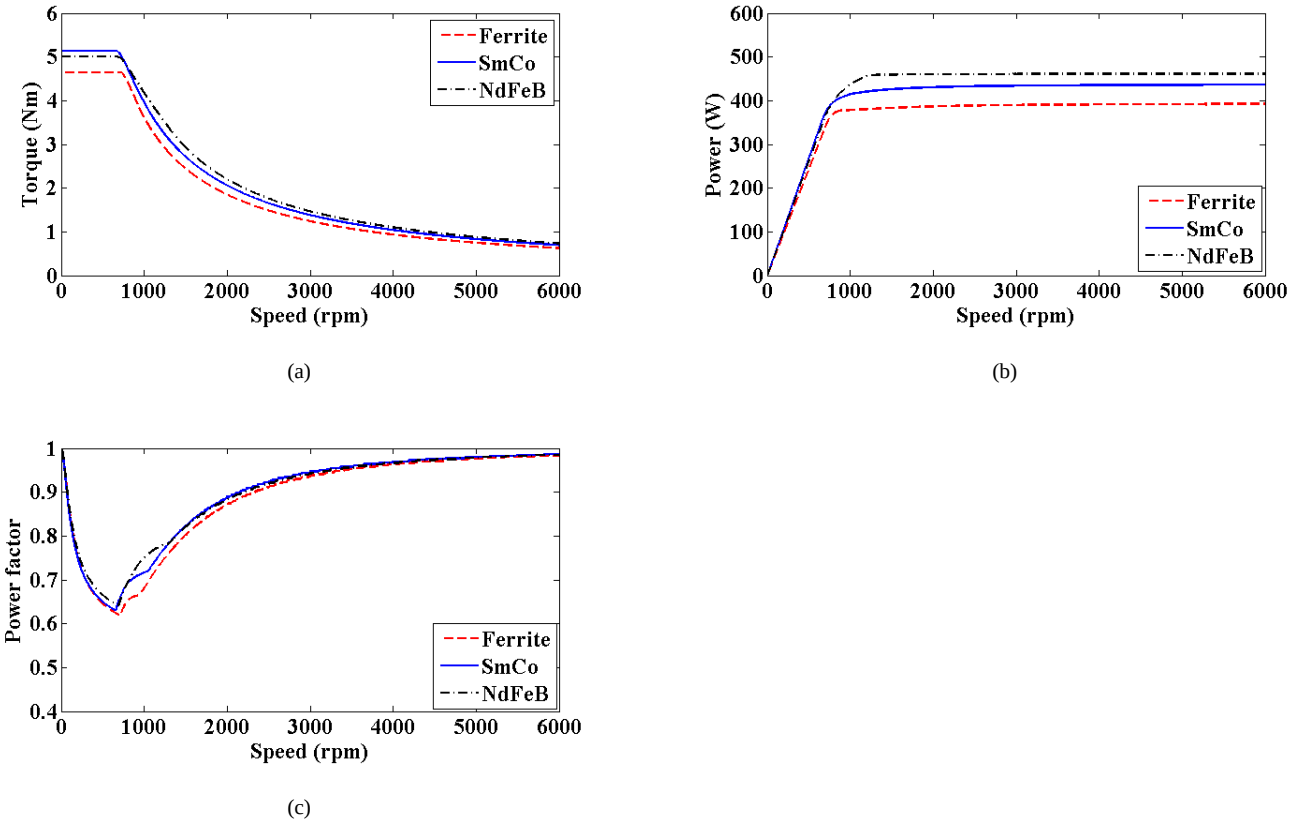

Fig. 9 Torque, power and power factor against speed characteristics for different PMs. The excitation current I_{ex} = 8A. (a) torque, (b) power, (c) power factor. The maximum armature RMS current is 7A.

5. EXPERIMENTAL VALIDATION

The 12-slot/10-pole prototype hybrid excited SFPM machine for experimental validation is the same as in [13]. The classic speed controller has been employed for MATLAB/Simulink simulation (the machine parameters such as open-circuit flux linkage, self and mutual inductances have been obtained using 2D FE calculations) while the dSPACE based programs have been developed for real-time control of the hybrid excited SFPM machine during tests. Three armature phases of the machine are supplied by a Voltage Source Inverter (VSI). Meanwhile, the excitation is supplied by a DC current generator. The load torque is 2.5 Nm for both simulation and measurement, the predicted and measured armature currents, excitation currents and rotor mechanical speeds are compared in Fig. 10. Without torque transducer, it is difficult to measure the instantaneous torque, but the good agreement between predicted and measured results can still prove the accuracy of predictions. It is also worth mentioning that the torque separation using FP method can only be validated by FEM rather than by measurements. This is because it is impossible to maintain the same magnetic saturation level, particularly local saturations, during measurements when machine load conditions (operating points) have changed.

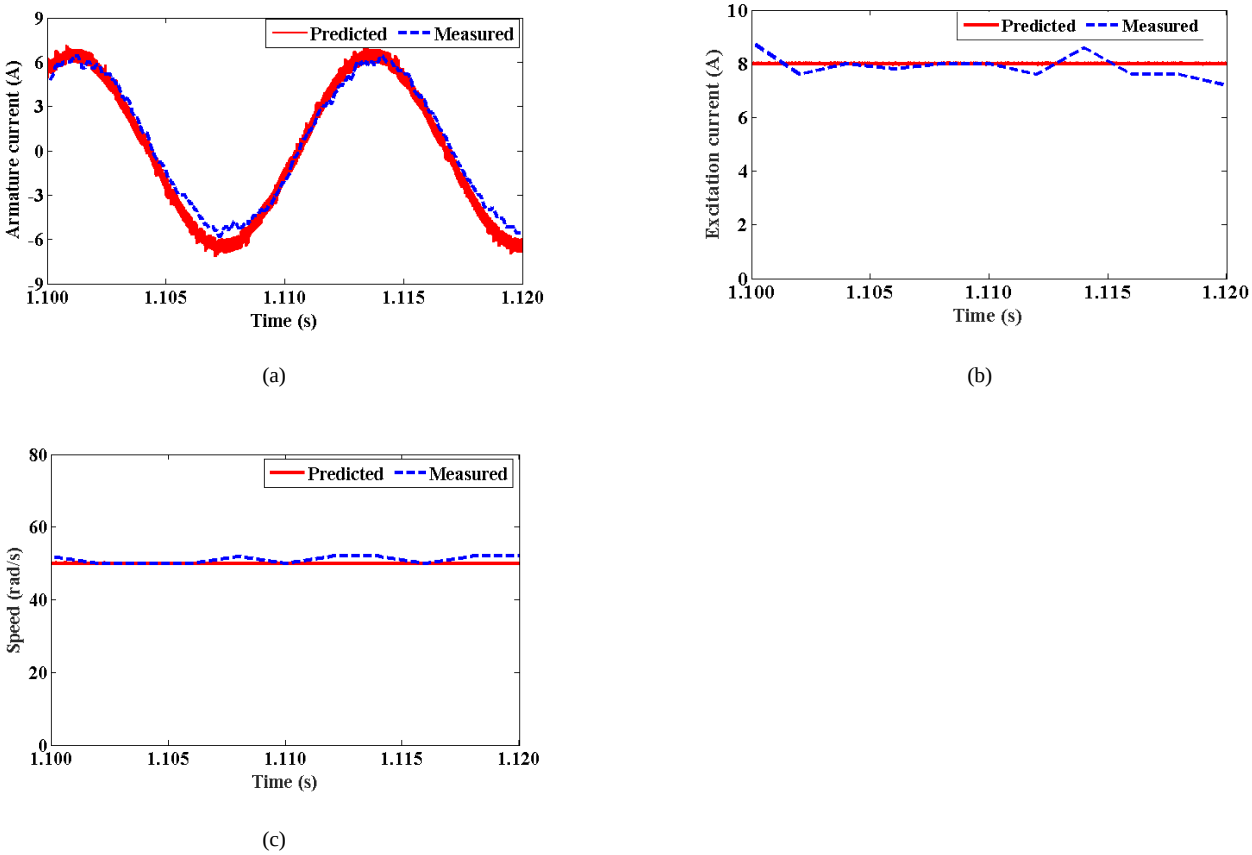

Fig. 10 Predicted and measured armature currents, excitation currents and rotor mechanical speeds. (a) armature currents, (b) excitation current and (c) rotor mechanical speeds. The load torque is 2.5 Nm.

6. CONCLUSION

This paper has employed the frozen permeability (FP) method to investigate the characteristics of hybrid excited switched flux permanent magnet (SFPM) machines. The flux separation has revealed an interesting phenomenon, i.e. the flux due to PMs reduces with the increase in excitation current. As a result, at high excitation current, the flux due to PMs hardly cross through the phase armature windings, leading to a phase flux linkage purely determined by the flux produced by field winding (excitation) only. This influence of excitation current on flux linkage due to PMs has also been reflected on the torque components. It is found that at high excitation current, the torque due to PMs only, similar to reluctance torque, is negligible compared to torque due to wound field only. However, it is worth mentioning that the FP method can only be validated by finite element method because during measurements, the magnetic saturation level cannot be maintained if machine operating points have changed.

Comparison in terms of torque components against excitation current, torque and power as well as power factor against rotor speed has been carried out for hybrid excited SFPM machines with different PMs. At an excitation current of 8A, the results have shown that with Ferrite, the machine can produce comparable maximum torque and also exhibit similar high speed performance

while with much lower magnet price level. This provides a useful alternative for applications requiring high torque and high speed performance while having strict cost constraints such as EV/HEV.

REFERENCES

[1] Zhao, W. X., Cheng, M., Hua, W., Jia, H. Y., and Cao, R. W.: 'Back-emf harmonic analysis and fault-tolerant control of flux-switching permanent-magnet machine with redundancy', IEEE Trans. Ind. Electron., May 2011, **58**, (5), pp. 1926-1935

[2] Zhao, W. X., Cheng M., Chau, K. T., Cao, R. W., and Ji, J. H.: 'Remedial injected-harmonic-current operation of redundant flux-switching permanent-magnet motor drives', IEEE Trans. Ind. Electron., Jan. 2013, **60**, (1), p. 151-159

[3] Aboelhassan, M. O. E., Raminosoa, T., Goodman, A., De Lillo, L., and Gerada, C.: 'Performance evaluation of a vector-control fault-tolerant flux-switching motor drive', IEEE Trans. Ind. Electron., Aug. 2013, **60**, (8), pp. 2997-3006

[4] Li, G. J., Ojeda, J., Hoang, E., and Gabsi, M.: 'Thermal-electromagnetic analysis of a fault-tolerant dual-star flux-switching permanent magnet motor for critical applications', IET Elec. Power Appl., Jul. 2011, **5**, (6), pp. 503-513

[5] Li, G. J., Ojeda, J., Hoang, E., Gabsi, M., and Lecrivain, M.: 'Thermal–electromagnetic analysis for driving cycles of embedded flux-switching permanent-magnet motors', IEEE Trans. Veh. Technol., Jan. 2012, **61**, (1), p p. 140-151

[6] Cheng, M., Chen, Z., Hua, W., and Zhang, J. Z.: 'Comparison of stator-mounted permanent-magnet machines based on a general power equation', IEEE Trans. Energy Convers., Dec. 2009, **24**, (4), pp. 826-834

[7] Chen, J. T., Zhu, Z. Q., Iwasaki, S., and Deodhar, R. P.: 'A novel E-core switched-flux PM brushless AC machine', IEEE Trans. Ind. Appl., May-Jun. 2011, **47**, (3), pp. 1273-1282

[8] Min, W., Chen, J. T., Zhu, Z. Q., Zhu, Y., Zhang, M., and Duan, G. H.: 'Optimization and comparison of novel E-core and C-core linear switched flux PM machines', IEEE Trans. Mag., Aug. 2011, **47**, (8), pp. 2134-2141

[9] Gaussens, B., Hoang, E., de la Barriere, O., Saint-Michel, J., Lecrivain, M., and Gabsi, M.: 'Analytical approach for air-gap modeling of field-excited flux-switching machine: no-load operation', IEEE Trans. Mag., Sept. 2012, **48**, (9), pp. 2505-2517

[10] Zhou, Y. J., and Zhu, Z. Q.: 'Comparison of wound-field switched-flux machines', IEEE Trans. Ind. Appl., Sept.-Oct. 2014, **50**, (5), pp. 3314-3324

[11] Rao, J., and Xu, W.: 'Modular stator high temperature superconducting flux-switching machines', IEEE Trans. Appl. Supercond., Oct. 2014, **24**, (5), pp. 1-5

[12] Chen, Z. H., Wang, B., Chen, Z., Yan, Y.G.: 'Comparison of flux regulation ability of the hybrid excitation doubly salient machines', IEEE Trans. Ind. Electron., Jul. 2014, **61**, (7), pp. 3155-3166

[13] Hoang, E., Lecrivain, M., and Gabsi, M.: 'A new structure of a switching flux synchronous polyphased machine with hybrid excitation', In 2007 European Conference on Power Electronics and Applications, 2-5 Sept. 2007

[14] Hoang, E., Hlioui, S., Lecrivain, M., and Gabsi, M.: 'Experimental comparison of lamination material case of switching flux synchronous machine with hybrid excitation', In 13th European Conf. Power Electron. Appl. (EPE); 8-10 Sep. 2009

[15] Hoang, E., Lecrivain, M., and Gabsi, M.: 'Flux-swiching dual excitation electrical machine', United states patent 7,868,506 B2. Jan. 11. 2011

[16] Hua, W., Cheng, M., and Zhang, G.: 'A novel hybrid excitation flux-switching motor for hybrid vehicles', IEEE Trans. Mag. 2009, **45**, (10), pp. 4728-4731

[17] Zhang, G., Hua, W., Cheng, M., Zhang, J. Z., and Jiang, W.: 'Investigation of an improved hybrid-excitation flux switching brushless machine for HEV/EV applications', In 2014 IEEE Energy Conversion Congress and Exposition (ECCE), 14-18

Sep. 2014, Pittsburgh, PA, USA. pp. 5852-5857

[18] Chen, J. T., Zhu, Z. Q., Iwasaki, S., Deodhar, R. P.: 'A novel hybrid-excited switched-flux brushless ac machine for EV/HEV applications', IEEE Trans. Veh. Technol., May 2011, **60**, (4), pp. 1365-1373

[19] Gaussens, B., Hoang, E., Lecrivain, M., Manfe, P., and Gabsi, M.: 'A hybrid-excited flux-switching machine for high-speed dc-alternator applications', IEEE Trans. Ind. Electron., June 2014, **61**, (6), pp. 2976-2989

[20] Hua, W., Yin, X. M., Zhang, G., Cheng, M.: 'Analysis of two novel five-phase hybrid-excitation flux-switching machines for electric vehicles', IEEE Trans. Mag., Nov. 2014, **50**, (11), pp. 1-5

[21] Bianchi, N., and Bolognani, S.: 'Magnetic models of saturated interior permanent magnet motors based on finite element analysis', In Proc. IEEE Ind. Appl. Conf., 12-15 Oct. 1998, St. Louis, MO, USA. pp. 27-34

[22] Ionel, D. M., Popescu, M., McGilp, M. I., Miller, T. J. E., and Dellinger, S. J.: 'Assessment of torque components in brushless permanent-magnet machines through numerical analysis of the electromagnetic field', IEEE Trans. Ind. Appl., Sept.-Oct. 2005, **41**, (5), pp. 1149-1158

[23] Azar, Z., Zhu, Z. Q., and Ombach, G.: 'Influence of electric loading and magnetic saturation on cogging torque, back-EMF and torque ripple of PM machines', IEEE Trans. Magn., Oct. 2012, **48**, (10), pp. 2650-2658

[24] Chu, W. Q., and Zhu, Z. Q.: 'Average torque separation in permanent magnet synchronous machines using frozen permeability', IEEE Trans. Mag., Mar. 2013, **49**, (3), pp. 1202-1210

[25] Chen, J. T., Zhu, Z. Q., Thomas, A. S., and Howe, D.: 'Optimal combination of stator and rotor pole numbers in flux-switching PM brushless AC machines', In International Conference on Electrical Machines and Systems (ICEMS), 17-20 Oct. 2008, Wuhan, China. pp. 2905-2910

[26] Walker, J. A., Dorrell, D. G., Cossar, C.: 'Flux-linkage calculation in permanent-magnet motors using the frozen permeabilities method', IEEE Trans. Magn., Oct. 2005, **41**, (10), pp. 3946-3948

[27] Chu, W. Q., and Zhu, Z. Q.: 'On-load cogging torque calculation in permanent magnet machines' IEEE Trans. Magn., June 2013, **49**, (6), pp. 2982-2989

[28] Dupas, A., Hoang, E., Hlioui, S., Gaussens, B., Lecrivain, M., and Gabsi, M.: 'Performances of a hybrid excited flux-switching dc-alternator: analysis and experiments', In Proceedings of the 2014 International Conference on Electrical Machines (ICEM), 2-5 Sep. 2014, Berlin, Germany. pp. 2632-2637

[29] Pothi, N., and Zhu, Z. Q.: 'A new control strategy for hybrid-excited permanent magnet machines without the requirement of machine parameters', In The 7th IET International Conference on Power Electronics, Machines and Drives, PEMD2014, 8 - 10 Apr. 2014

[30] Kwak, S. Y., Kim, J. K., and Jung, H. K.: 'Characteristic analysis of multilayer-buried magnet synchronous motor using fixed permeability method', IEEE Trans. Energy Convers., Sept. 2005, **20**, (3), pp. 549-555

[31] Qi, G., Chen, J. T., Zhu, Z. Q., Howe, D., Zhou, L. B., and Gu, C. L.: 'Influence of skew and cross-coupling on flux-weakening performance of permanent-magnet brushless ac machines', IEEE Trans. Mag., May 2009, **45**, (5), pp. 2110-2117

[32] Mohan, N., Undeland, T. M., and Robbins, W. P.: 'Power Electronics' (New York, Springer, 1995)